Functionalization of Carbon Nanotubes with Derivatized Polyimide

Darron Hill,[†] Yi Lin,[†] Liangwei Qu,[†] Alex Kitaygorodskiy,[†] John W. Connell,[‡] Lawrence F. Allard,[§] and Ya-Ping Sun*,[†]

Department of Chemistry and Laboratory for Emerging Materials and Technology, Clemson University, Clemson, South Carolina 29634-0973, Advanced Materials and Processing Branch, NASA Langley Research Center, Mail Stop 226, Hampton, Virginia 23681-2199, and High Temperature Materials Laboratory, Oak Ridge National Laboratory, Oak Ridge, Tennessee 37831-6062

Received May 2, 2005; Revised Manuscript Received July 4, 2005

ABSTRACT: Single-walled and multiple-walled carbon nanotubes were functionalized with derivatized polyimide for the homogeneous dispersion of the nanotubes. For the functionalization, the nanotube-bound carboxylic acids derived from the surface defects were targeted for esterification reactions with pendant hydroxyl groups in the derivatized polyimide. The functionalized nanotube samples, readily soluble in several common organic solvents, were thoroughly characterized by a series of instrumental techniques including NMR in both solution phase and solid state, optical absorption, Raman, thermogravimetric analysis, and microscopy methods. The results were consistent with well-dispersed nanotubes functionalized by the polyimide, and also with the expectation that the nanotube electronic properties were largely preserved in the specific mode of functionalization. The presumed formation of ester linkages in the functionalized samples was supported by the results from chemical defunctionalization. The potential applications of the polyimide-functionalized carbon nanotubes and the demonstrated functionalization strategy are discussed.

Introduction

The dispersion of single-walled (SWNT) and multiple-walled (MWNT) carbon nanotubes into polymeric materials has received much attention for both fundamental and practical interests in polymeric/carbon nanocomposites.[1,2] The solubilization of carbon nanotubes has been identified as an effective means to disperse the nanotubes homogeneously in wet processing.[3−10] Covalent functionalization methods based on either the side-wall addition or the nanotube-bound carboxylic acid moieties have commonly been used for the desired solubilization. For the latter in particular, where the carboxylic acids are from the oxidation of the nanotube surface defects, the facile attachment of a variety of oligomeric and polymeric functionalities to carbon nanotubes has been demonstrated.[11−13]

In the use of soluble functionalized carbon nanotubes for polymeric nanocomposites, an important and sometimes critical issue is the compatibility with the composite matrix polymer by the covalently attached functional groups responsible for "dragging" the nanotubes into solution. As suggested by Sun and co-workers,[3,7a,8] a logical approach to ensure compatibility is to use functional groups that are structurally identical or very similar to the matrix polymer. For poly(vinyl alcohol) (PVA), as an example, excellent compatibility has been achieved with the use of PVA-functionalized carbon nanotubes.[7]

Aromatic polyimides are high-performance polymers, particularly attractive for their high thermal stability, low color, flexibility, and processibility.[14] Nanocomposites of polyimides with carbon nanotubes are considered as being promising for many applications, especially as lightweight materials for uses in space.[8,9,15] For the dispersion of carbon nanotubes into the soluble aromatic polyimide poly[3′,3"-(1,3-bisphenoxybenzene)-*alt*-*N*,*N*′-(4,4′-hexafluoroisopropylidene diphthalimide)] (CP-2), Qu et al. functionalized the nanotubes with an amine-terminated oligomeric analogue of the polyimide.[8] Here we report a somewhat different approach by introducing pendant hydroxyl groups into some repeating units in the polyimide for esterification reactions with the nanotube-bound carboxylic acids. The resulting polyimide-functionalized carbon nanotubes were found to be soluble in the same solvents as the parent polyimide. A significant advantage with this approach is that the functionalized nanotube samples can be used directly for polyimide-carbon nanocomposites of relatively higher nanotube contents.

Experimental Section

Materials. 3,5-Diaminobenzyl alcohol dihydrochloride (97%) and 4,4′-(hexafluoroisopropylidene)diphthalic anhydride (99%) were purchased from Aldrich, 1,3-bis(3-aminophenoxy)benzene from TCI, and *N*,*N*′-dicyclohexylcarbodiimide (DCC, 99%), 4-(dimethylamino)pyridine (DMAP, 99%), aniline, 1-hydroxybenzotriazole (BtOH, 98%), sodium hydride (NaH, 60% dispersed in mineral oil), and 1-methyl-2-pyrrolidinone (NMP) from Acros. Toluene, dimethyl formamide (DMF), and other solvents were obtained from Mallinckrodt. NMP and DMF were distilled over calcium hydride, and THF over sodium before use. Deuterated solvents for NMR measurements were purchased from Cambridge Isotope Laboratories.

SWNT and MWNT samples were supplied by Carbon Solutions Inc. and Nanostructured and Amorphous Materials Inc., respectively. The ^{13}C-enriched SWNT sample was synthesized in house by the laser ablation method. The ablation target was made of a mixture of powdery ^{13}C and graphite as the carbon source and Ni/Co as catalysts.[16] The atomic content of ^{13}C in the enriched SWNT sample was 33%, estimated from the Raman analysis.[17] The nanotube samples were purified by a combination of thermal oxidation and oxidative acid treatments. In a typical experiment, a nanotube sample (1 g)

* Corresponding author.
† Clemson University.
‡ NASA Langley Research Center.
§ Oak Ridge National Laboratory.

10.1021/ma0509210 CCC: $30.25
Published on Web 08/13/2005

was heated in a furnace to 300 °C in air for 30 min. After the thermal oxidation treatment, the remaining sample was suspended in an aqueous HNO_3 solution (2.6 M) and refluxed for 24 h. Upon centrifuging at 1000 g, the supernatant was discarded and the remaining solids were washed with deionized water until neutral pH and dried under vacuum.

Measurements. NMR measurements were performed on a JEOL Eclipse +500 NMR spectrometer and a Bruker Avance 500 spectrometer, with the latter being equipped with a 4 mm magic angle spinning (MAS) probe-head for solid samples. Optical absorption spectra were recorded on a Shimadzu UV3100 spectrophotometer, and Raman spectra were obtained on a Jobin Yvon T64000 Raman spectrometer equipped with a 35 mW He−Ne laser source for 632.8 nm excitation and a CCD detector. Scanning (SEM) and transmission (TEM) electron microscopy images were acquired on a Hitachi S-4700 field-emission SEM system and a Hitachi HF-2000 TEM system, respectively. Atomic force microscopy (AFM) analysis was conducted on a Molecular Imaging PicoPlus system equipped with a multipurpose scanner. The height profile analyses were assisted by using the SPIP software distributed by Image Metrology.

Derivatized Polyimide with Pendant Hydroxyl Groups (PI_{OH}). A solution of 1,3-bis(3-aminophenoxy)benzene (529 mg, 1.74 mmol) and 3,5-diaminobenzyl alcohol dihydrochloride (94.5 mg, 0.43 mmol) in dry NMP (10 mL) was prepared in a sealed round-bottom flask under N_2 protection, and the solution was cooled in an ice bath for 15 min. To the solution was added 4,4′-(hexafluoroisopropylidene)diphthalic anhydride (1 g, 2.23 mmol), and the mixture was stirred at 0 °C for 6 h. Aniline (10 mg, 0.11 mmol) was added, and the resulting mixture was warmed back to room temperature and stirred for 30 h. Toluene (5 mL) was added, and the flask containing the reaction mixture was attached to a condenser with a toluene-filled Dean−Stark trap and then heated to 150 °C. When the amount of water removed by the azeotrope reached ~0.05 mL (measured via microsyringe), the reaction mixture was cooled to room temperature. Upon the removal of toluene and some NMP on a rotary evaporator, the mixture was added dropwise into bulk methanol with vigorous stirring. The solid precipitate was filtered, subjected to Soxhlet extraction with methanol for 6 h, and then dried under vacuum at 60 °C. PI_{OH} was obtained as a slightly yellowish powder (1.29 g. 87% yield). ^{1}H NMR (500 MHz, DMSO-d_6) δ 8.09 (d), 7.93 (s), 7.74−7.62 (m), 7.49 (d), 7.43−7.33 (m), 7.27−7.09 (m), 6.90−6.69 (m), 5.51 (s), 4.60 (s) ppm. ^{13}C NMR (125 MHz, DMSO-d_6) δ 166.4, 166.3, 157.9, 156.9, 137.8, 136.3, 133.6, 133.1, 132.5, 131.9, 130.9, 127.3, 125.8, 124.9, 124.2, 123.2, 122.7, 120.5, 118.9, 118.1, 114.7, 110.2, 65.1 (m), 62.7 ppm. Gel permeation chromatography (GPC, Perkin-Elmer PLgel 10 μ Mixed Columns (×3), THF as solvent, linear polystyrene standards): $M_w \sim 10\,800$ and polydispersity index ~2.2.

Nanotube Functionalization. In a typical reaction, DCC (400 mg, 1.2 mmol), DMAP (66 mg, 0.3 mmol), and BtOH (130 mg, 0.6 mmol) were dissolved in DMF (25 mL). To the solution was added a purified SWNT sample (166 mg), and the mixture was sonicated (VWR Aquasonic 150 HT) for 2 h. A DMF solution (10 mL) of PI_{OH} (1.6 g) was added, and the resulting mixture was sonicated for another 48 h. Following the removal of DMF on a rotary evaporator, the crude product was redissolved in THF (~15 mL) via brief sonication for dialysis in a PVDF membrane tubing (cutoff molecular weight ~ 250 000) against THF for 3 days. The mixture was centrifuged at 3000 g to separate the dark-colored supernatant containing the PI_{OH}-functionalized SWNTs (PI_{OH}−SWNT) from the insoluble residue (unfunctionalized and underfunctionalized nanotubes[3,11]).

The same procedure was applied to the functionalization of ^{13}C-enriched SWNTs and MWNTs with PI_{OH}. The resulting functionalized nanotube samples (PI_{OH}−^{13}C-SWNT and PI_{OH}−MWNT) were also black solids.

Chemical Defunctionalization. A PI_{OH}−SWNT sample (37 mg) was dissolved in THF (6 mL) to form a dark-colored but homogeneous solution. To the solution was added NaH (80 mg, 3.33 mmol), and the mixture was refluxed under N_2 protection for 12 h and then cooled to ambient temperature. To the mixture was carefully added water (~1.5 mL) to quench the reaction, followed by heating the mixture again to reflux for another hour. The reaction mixture became a slightly yellowish solution with black precipitates. The precipitates were recovered via centrifuging and washed thoroughly with hexane and water.

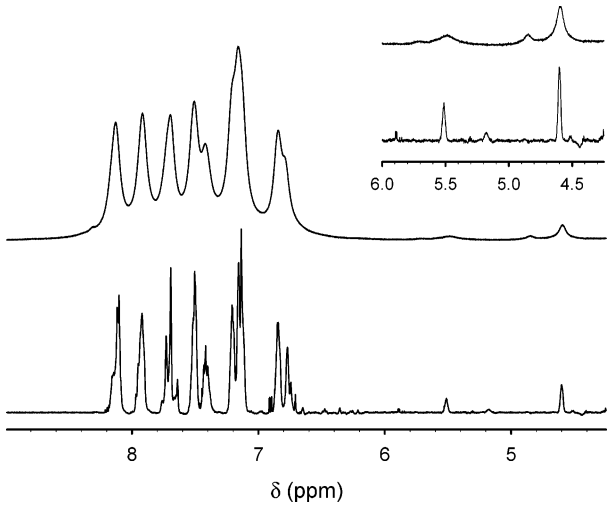

Figure 1. ^{1}H NMR spectrum of PI_{OH}−SWNT (top) compared with that of the parent PI_{OH} polymers (bottom) in DMSO-d_6 solutions. Shown in the inset is an enlarged view of the region containing OH and benzylic CH_2 proton signals.

Results and Discussion

The pendant hydroxyl groups (benzylic alcohols) in PI_{OH} were required for the functionalization of carbon nanotubes. In the ^{1}H NMR spectrum (Figure 1), the hydroxyl proton and the benzylic protons (Scheme 1)

Scheme 1

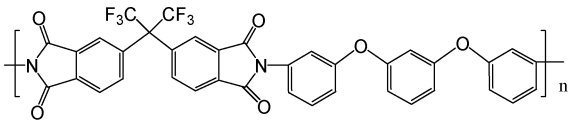

CP-2

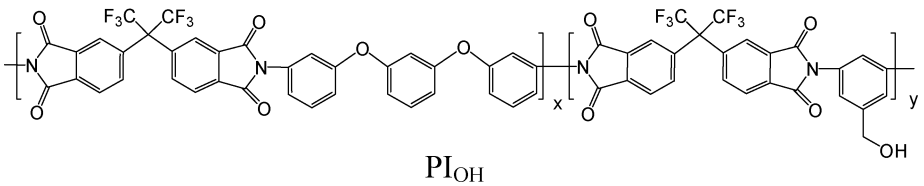

PI_{OH}

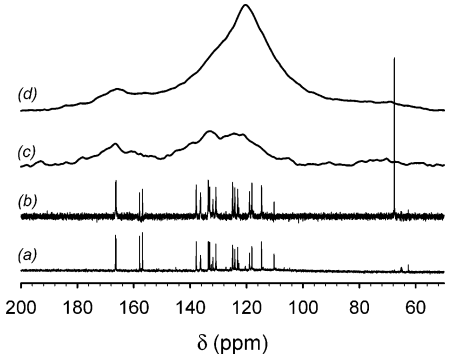

Figure 2. ^{13}C NMR spectra of (a) PI_{OH} and (b) PI_{OH}−SWNT in DMSO-d_6 solutions, and (c) the solid-state MAS ^{13}C NMR cross-polarization (CP) and (d) direct-polarization (DP) spectra of PI_{OH}−^{13}C−SWNT.

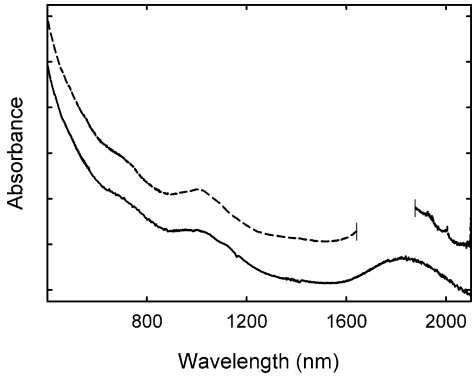

Figure 3. Optical absorption spectra of PI_{OH}−SWNT as solid-state film on glass (—) and in room-temperature DMF solution (- - -), for which the solvent background in the missing region was too strong to be corrected.

were identified by signals at 5.51 and 4.60 ppm, respectively, with the correct ratio 1:2 for their signal integrations. The labile nature of the 5.51 ppm signal was made evident by its disappearance upon the addition of deuterated methanol to the NMR sample solution. According to the relative ^1H NMR signal integrations, the benzyl alcohol mole fraction in PI_{OH} was estimated to be ∼7% (averaging one −OH moiety per seven repeating units).

For PI_{OH}−SWNTs in solution, the NMR characterization was carried out in deuterated DMSO. The solution-phase ^1H NMR spectrum of PI_{OH}−SWNT is compared with that of PI_{OH} in Figure 1. For the nanotube-attached PI_{OH}, the proton signals are much broader, as commonly observed in the NMR characterization of solubilized carbon nanotubes. Such signal broadening effect may be attributed to the high molecular weight and low mobility of the nanotube.[18] Except for being broader, the aromatic proton peaks in SWNT-attached PI_{OH} are generally similar to those in free PI_{OH} (Figure 1). However, there are characteristic changes in the proton signals of the pendant benzylic alcohol. After the polymer attachment to nanotubes, the hydroxyl and benzylic proton signals each split into two separate peaks. This might be a result of these protons being close to the nanotube surface. It has been reported that protons located in close proximity to the point of attachment to the nanotube surface may be shifted from their original positions in NMR spectra.[19−21] In addition, the partial transformation of the alcohols into esters linking the nanotubes results in the loss of some hydroxyl protons, as reflected by the change in the hydroxyl-to-benzylic ratio from 1:2 before functionalization to 0.76:2 post functionalization. In other words, about a quarter of the hydroxyl groups in the starting PI_{OH} were consumed in the functionalization of SWNTs for the formation of ester linkages. The solution-phase ^{13}C NMR spectrum of PI_{OH}−SWNT is also largely similar to that of the starting PI_{OH} polymer. The pendant methylene carbon signal at 62.7 ppm for nanotube-attached PI_{OH} has a lower intensity (Figure 2), consistent with the partial transformation of the benzylic alcohols in the functionalization. However, the expected ester formation is not clear in ^{13}C NMR, due probably to several technical factors, including the relatively low carbonyl population in generally inhomogeneous environments causing signal broadening.

In a quantitative ^1H NMR measurement of PI_{OH}−SWNT in solution, 4,4′-dimethoxybenzophenone was used as an internal standard for observed signal intensities. Based on the signal integrations in reference to the standard, the PI_{OH} content in the sample was estimated to be about 65% (w/w), namely that the nanotube content in the sample should be approximately 35% (w/w).

The nanotube carbons in PI_{OH}-functionalized SWNTs were probed by solid-state MAS ^{13}C NMR with the use of the ^{13}C-enriched sample (PI_{OH}−^{13}C-SWNT). In the cross-polarization (CP) spectrum shown in Figure 2, the contribution from nanotube carbons is negligible because of the lack of proton decoupling. The signals at 110−140 and 166 ppm may be assigned to the imide aromatic and carbonyl carbons, respectively. However, in the direct polarization (DP) spectrum (Figure 2), the nanotube carbon signal at ∼120 ppm is predominant.[16,22−25] The peak is somewhat unsymmetric, with a shoulder toward the downfield. The shoulder could simply be attributed to contributions from the overlapping aromatic carbon signals found in the CP spectrum, though other possibilities might also be considered in light of the recent ^{13}C NMR results on nanotube carbons in simpler functionalized nanotube samples.[25] Further solid-state and even solution-phase investigations of the nanotube carbons in the functionalized samples will be pursued.

Both PI_{OH}−SWNT and PI_{OH}−MWNT form colored solutions in DMF (stable at least in months), and the solution color ranges from light brown to black with increasing concentration. Shown in Figure 3 are optical absorption spectra of PI_{OH}−SWNTs, where the spectrum in DMF solution is generally similar to that in the solid-state deposited on a glass slide. The absorption bands at ∼1800 nm and ∼1000 nm are characteristic of the electronic transitions associated with the first (S_{11}) and second (S_{22}) pairs of van Hove singularities in the density of states for the semiconducting SWNTs, and the band at ∼700 nm corresponds to the absorption of the metallic SWNTs (M_{11}). The results suggest that the electronic structures of SWNTs are preserved upon the functionalization targeting the nanotube surface defect sites. For PI_{OH}−MWNT, as expected,[11,18] the absorption spectra are featureless curves with decreasing absorptivities toward longer wavelengths (similar to that of a MWNT suspension, except for less scattering).

Several microscopy techniques were applied to the characterization of PI_{OH}−SWNT and PI_{OH}−MWNT. The relatively larger sizes of MWNTs made their imaging by TEM more straightforward. As shown in Figure 4, the MWNTs in the functionalized sample were well-

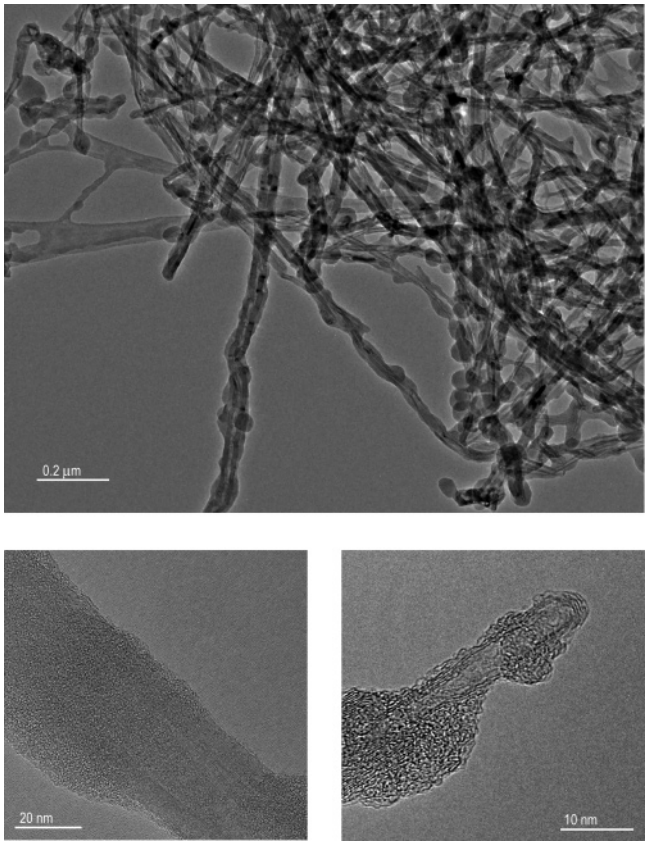

Figure 4. TEM images of the PI_{OH}–MWNT sample at lower (top) and higher (bottom) magnifications.

dispersed, with the nanotube surface coated presumably by the polyimide polymers.[26] The area imaging of the functionalized SWNTs by TEM was proven to be considerably more difficult, probably due to the relatively low contrast between the dispersed nanotubes and the polymeric functional groups. At a higher resolution, the TEM image in Figure 5a suggests that the SWNTs in the functionalized sample were dispersed either individually or as thin bundles. This is supported by results from the AFM analysis. The specimen for the analysis was prepared by the spin-casting of a diluted solution of PI_{OH}–SWNT onto mica surface. The AFM image shown in Figure 5b is consistent with the presence of abundant functionalized SWNTs, and the height profile acquired along the line in the image (Figure 5b,c) is also consistent with the presence of individual or thin bundles of functionalized SWNTs (feature sizes of 1–18 nm).

The good dispersion of nanotubes in the functionalized samples was also reflected by the overwhelming luminescence interference in resonance Raman measurements (Figure 6). No such interference was found in the simple polymer-nanotube mixtures. This was not surprising because such interference has been widely observed in functionalized carbon nanotube samples (no PI_{OH} absorption at the laser wavelength 633 nm, thus no fluorescence from the polymer). The luminescence may be attributed to well-passivated nanotube surface defects,[11,27,28] namely that structural defects on nanotubes may act as traps for the photoexcitation energy, and upon stabilization by the functional groups these energy trapping sites may become strongly luminescent. As discussed in the literature,[11] there is strong experimental evidence suggesting that the functionalization is required for the observation of the nanotube-defect-

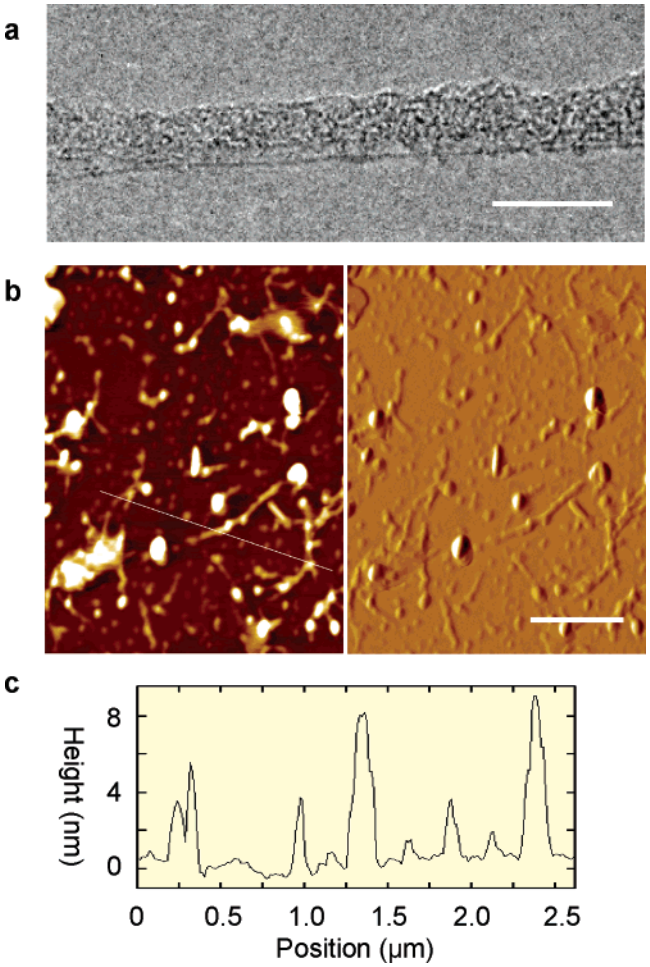

Figure 5. (a) TEM image (scale bar = 10 nm) and (b) typical AFM topography (left) and amplitude (right) images of the PI_{OH}–SWNT sample (scale bar = 1 μm), and (c) the height profile across the line in the AFM topography image.

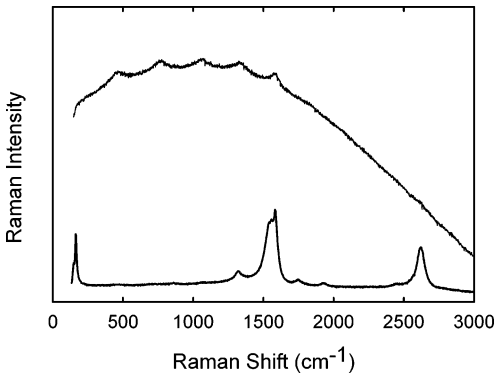

Figure 6. Raman spectra of the PI_{OH}–SWNT sample before (upper curve) and after (lower curve) the chemical defunctionalization.

derived luminescence and that a better dispersion of nanotubes in their functionalization enhances the luminescence and, consequently, results in more significant interference in resonance Raman measurements. Such a direct correspondence between luminescence enhancement and improved nanotube dispersion is understandable because of the known inter-tube quenching effect associated with the bundling of the nanotubes.[11,29] Typically, a simple validation of the argument is to measure the Raman spectrum after the removal of functional groups via thermal defunctionalization in a slow TGA scan.[3,7a,30] However, the PI_{OH} species

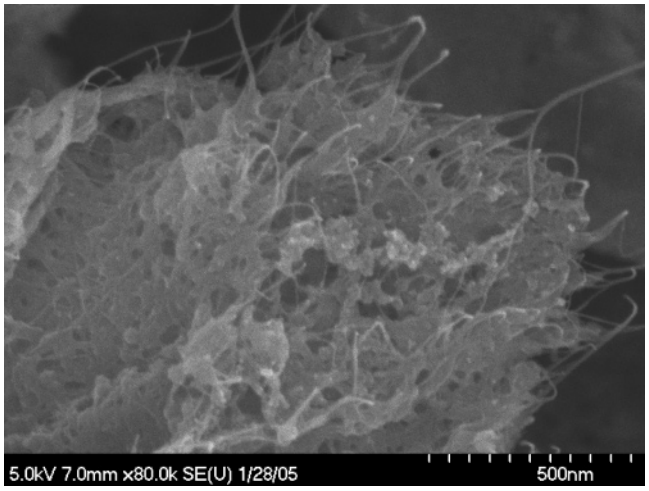

Figure 7. Typical SEM image of the insoluble precipitate obtained from the chemical defunctionalization of the PI_{OH}−SWNT sample.

attached to the nanotubes could not be removed thermally because of their carbonization. In fact, the TGA traces of the PI_{OH}−SWNT sample and neat PI_{OH} are similar, both showing a large amount of residues at high temperatures (to 1,000 °C in nitrogen). Thus, the defunctionalization to remove at least some of the nanotube-attached PI_{OH} species was accomplished chemically via hydrolysis (see below).[31] The Raman spectrum of the chemically defunctionalized PI_{OH}−SWNT sample exhibits the characteristic SWNT peaks at 164 cm^{-1} (radial breathing mode), 1317 cm^{-1} (D-band), 1582 cm^{-1} (G-band), and 2624 cm^{-1} (D*-band). The unsymmetrical Breit−Wigner−Fano (BWF) line shape of the G-band is probably due to the excitation (633 nm) into the M_{11} absorption band.[32]

The chemical defunctionalization also served the purpose of mechanistic elucidation. The functionalization chemistry for attaching PI_{OH} to nanotubes was designed specifically for the formation of ester linkages. The chemical defunctionalization via hydrolysis (or hydrogenolysis, to be more exact) was unique to the PI_{OH}-functionalized nanotube samples discussed here, not available to those based on amide linkages reported previously.[8] The facile defunctionalization reaction resulted in the precipitation of dark-colored solids, which were mostly carbon nanotubes with some PI_{OH} species still remaining on the nanotube surface according to the SEM analysis. As shown in Figure 7, the recovered sample from the chemical defunctionalization of PI_{OH}−SWNT appeared more like a composite material. There was surface charging effect during the SEM analysis, indicative of the presence of nonconductive materials. The incompleteness in the removal of PI_{OH} from nanotubes in the chemical defunctionalization was probably due to the progressively inhomogeneous nature of the hydrogenolysis reaction. On the other hand, the precipitation of the nanotubes from the solution in the chemical defunctionalization was nearly quantitative. The supernatant separated from the precipitates became light-colored (instead of the black color before the reaction), as reflected in the comparison of optical absorption spectra before and after the chemical defunctionalization (Figure 8).

The use of derivatized polymer or copolymer with pendant hydroxyl groups as minor units is apparently an effective strategy in the functionalization of carbon

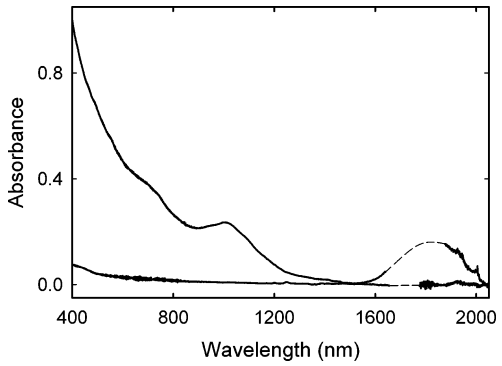

Figure 8. UV-vis/near-IR absorption spectra of the PI_{OH}−SWNT sample in DMF solution (upper curve) and the remaining supernatant after the chemical defunctionalization reaction (lower curve).

nanotubes. The structural similarity between the derivatized polymer or copolymer and the parent polymer typically guarantees full compatibility of the functionalized carbon nanotubes with the matrix polymer in the fabrication of nanocomposites. Indeed, the soluble PI_{OH}−SWNT and PI_{OH}−MWNT samples are miscible with the parent CP-2 polymer in any proportions. For example, the CP-2 polyimide-SWNT nanocomposite of 25 wt % nanotube content can easily be prepared. In fact, the PI_{OH}−SWNT sample itself (nanotube content ~35 wt %) forms a black-colored thin film. More investigations are required to evaluate the properties of these nanocomposite materials.

Since the polymer attachment is through the nanotube surface defect sites, the electronic structures of the nanotubes as reflected by the band-gap transitions are largely preserved in the functionalization. This is valuable to the use of carbon nanotubes in polymeric nanocomposites. Interestingly, however, the CP-2 polyimide is a relatively nanotube-affinitive polymer, similar to or even better than conductive polymers rich in aromatic moieties,[33] but the nanotube electronic transitions are little affected despite the expectation for significant polymer−nanotube interactions. It has been established recently that planar molecules of multiple aromatic rings such as pyrene and porphyrin may interact noncovalently with SWNTs to the extent of diminishing the characteristic S_{11} and S_{22} transitions.[34] Thus, the arrangement of aromatic moieties in the molecules for functionalization appears to play an important role in determining the kind of interactions with nanotubes. The widely assumed "wrapping" of nanotubes by polymers with linearly arranged small aromatic moieties apparently represents a mode of interaction that is friendly to preserving the electronic properties of carbon nanotubes.

There is also the advancement in the understanding of the functionalization mechanism. The results presented here suggest that the formation of ester linkages is responsible for the polymer attachment to carbon nanotubes. Since minor hydroxyl moieties are present in many polymers or can be introduced relatively conveniently without significantly changing the polymer structures, this strategy may find increasing applications in the functionalization and solubilization of carbon nanotubes. Finally, according to preliminary results from a systematic investigation in progress, the functionalized carbon nanotubes are much better dispersed than their unfunctionalized counterparts in polymeric nanocomposites.

Acknowledgment. We thank P. Pathak, B. Zhou, Dr. B. Chen, and M. Veca for experimental assistance. Financial support from NASA through a cross-enterprise NRA grant and, in part, from the NSF, is gratefully acknowledged. D.H. was an awardee of the NASA Graduate Student Researcher Program (GSRP). Research at Oak Ridge National Laboratory was sponsored by the Assistant Secretary for Energy Efficiency and Renewable Energy, Office of FreedomCAR and Vehicle Technologies, as part of the HTML User Program, managed by UT-Battelle LLC for DOE (DE-AC05-00OR22725).

Supporting Information Available: Figures showing the TGA traces of PI_{OH} and PI_{OH}−SWNT, ^1H NMR of a simple mixture of PI_{OH} and SWNTs, and optical absorption spectrum of purified SWNTs. This material is available free of charge via the Internet at http://pubs.acs.org.

References and Notes

(1) (a) Ajayan, P. M. *Chem. Rev.* **1999**, *99*, 1787−1799. (b) Baughman, R. H.; Zakhidov, A. A.; de Heer, W. A. *Science* **2002**, *297*, 787−792. (c) Andrews, R.; Jacques, D.; Qian, D.; Rantell, T. *Acc. Chem.* Res. **2002**, *35*, 1008−1017.

(2) Fu, K.; Sun, Y.-P. *J. Nanosci. Nanotechnol.* **2003**, *3*, 351−364.

(3) (a) Hill, D. E.; Lin, Y.; Rao, A. M.; Allard, L. F.; Sun, Y.-P. *Macromolecules* **2002**, *35*, 9466−9471. (b) Hill, D. E.; Lin, Y.; Allard, L. F.; Sun, Y.-P. *Int. J. Nanosci.* **2002**, *1*, 213−221.

(4) Viswanathan, G.; Chakrapani, N.; Yang, H.; Wei, B.; Chung, H.; Cho, K.; Ryu, C. Y.; Ajayan, P. M. *J. Am. Chem. Soc*. **2003**, *125*, 9258−9259.

(5) Qin, S.; Qin, D.; Ford, W. T.; Resasco, D. E.; Herrera, J. E. *J. Am. Chem. Soc.* **2004**, *126*, 170−176.

(6) Kong, H.; Gao, C.; Yan, D. *J. Am. Chem. Soc.* **2004**, *126*, 412−413.

(7) (a) Lin, Y.; Zhou, B.; Fernando, K. A. S.; Liu, P.; Allard, L. F.; Sun, Y.-P. *Macromolecules* **2003**, *36*, 7199−7204. (b) Paiva, M. C.; Zhou, B.; Fernando, K. A. S.; Lin, Y.; Kennedy, J. M.; Sun, Y.-P. *Carbon* **2004**, 2849−2854.

(8) Qu, L. W.; Lin, Y.; Hill, D. E.; Zhou, B.; Wang, W.; Sun, X. F.; Kitaygorodskiy, A.; Suarez, M.; Connell, J. W.; Allard, L. F.; Sun, Y.-P. *Macromolecules* **2004**, *37*, 6055−6060.

(9) Smith, J. G.; Connell, J. W.; Delozier, D. M.; Lillehei, P. T.; Watson, K. A.; Lin, Y.; Zhou, B.; Sun, Y.-P. *Polymer* **2004**, *45*, 825−836.

(10) Gao, J. B.; Itkis, M. E.; Yu, A.; Bekyarova, E.; Zhao, B.; Haddon, R. C. *J. Am. Chem. Soc.* **2005**, *127*, 3847−3854.

(11) Sun, Y.-P.; Fu, K.; Lin, Y.; Huang, W. *Acc. Chem. Res.* **2002**, *35*, 1096−1104.

(12) Niyogi, S.; Hamon, M. A.; Hu, H.; Zhao, B.; Bhowmik, P.; Sen, R.; Itkis, M. E.; Haddon, R. C. *Acc. Chem. Res.* **2002**, *35*, 1105−1113.

(13) (a) Hirsch, A. *Angew. Chem., Int. Ed.* **2002**, *41*, 1853−1859. (b) Bahr, J. L.; Tour, J. M. *J. Mater. Chem.* **2002**, *12*, 1952−1958.

(14) Wilson, D.; Stenzenberger, H. D.; Hergenrother, P. M. *Polyimides*; Chapman & Hall: London, 1990.

(15) (a) Park, C.; Ounaies, Z.; Watson, K. A.; Crooks, R. E.; Smith, J. E., Jr.; Lowther, S. E.; Connell, J. W.; Siochi, E. J.; Harrison, J. S.; St. Clair, T. L. *Chem. Phys. Lett.* **2002**, *364*, 303−308. (b) Watson, K. A.; Ghose, S.; Delozier, D. M.; Smith, J. E., Jr.; Connell, J. W. *Polymer* **2005**, *46*, 2076−2085.

(16) Kitaygorodskiy, A.; Wang, W.; Xie, S. Y.; Lin, Y.; Fernando, K. A. S.; Qu, L.; Chen, B.; Sun, Y.-P. *J. Am. Chem. Soc*. **2005**, *127*, 7517−7520.

(17) Liu, L.; Fan, S. S. *J. Am. Chem. Soc.* **2001**, *123*, 11502−11503.

(18) Sun, Y.-P.; Huang, W.; Lin, Y.; Fu, K.; Kitaygorodskiy, A.; Riddle, L. A.; Yu, Y. J.; Carroll, D. L. *Chem. Mater.* **2001**, *13*, 2864−2869.

(19) Chen, J.; Liu, H.; Weimer, W. A.; Halls, M. D.; Waldeck, D. H.; Walker, G. C. *J. Am. Chem. Soc*. **2002**, *124*, 9034−9035.

(20) Holzinger, M.; Abraham, J.; Whelan, P.; Graupner, R.; Ley, L.; Hennrich, F.; Kappes, M.; Hirsch, A. *J. Am. Chem. Soc*. **2003**, *125*, 8566−8580.

(21) Ruther, M. G.; Frehill, F.; O'Brien, J. E.; Minett, A. I.; Blau, W. J.; Vos, J. G.; in het Panhuis, M. *J. Phys. Chem. B* **2004**, *108*, 9665−9668.

(22) Tang, X.-P.; Kleinhammes, A.; Shimoda, H.; Fleming, L.; Bennoune, K. Y.; Sinha, S.; Bower, C.; Zhou, O.; Wu, Y. *Science* **2000**, *288*, 492−494.

(23) Goze-Bac, C.; Latil, S.; Lauginie, P.; Jourdain, V.; Conard, J.; Duclaux, L.; Rubio, A.; Bernier, P. *Carbon* **2002**, *40*, 1825−1842.

(24) Peng, H.; Alemany, L. B.; Margrave, J. L.; Khabashesku, V. N. *J. Am. Chem. Soc.* **2003**, *125*, 15174−15182.

(25) Cahill, L. S.; Yao, Z.; Adronov, A.; Penner, J.; Moonoosawmy, K. R.; Kruse, P.; Goward, G. R. *J. Phys. Chem. B* **2004**, *108*, 11412−11418.

(26) Lin, Y.; Hill, D. E.; Bentley, J.; Allard, L. F.; Sun, Y.-P. *J. Phys. Chem. B* **2003**, *107*, 10453−10457.

(27) (a) Riggs, J. E.; Guo, Z.; Carroll, D. L.; Sun, Y.-P. *J. Am. Chem. Soc.* **2000**, *122*, 5879−5880. (b) Sun, Y.-P.; Zhou, B.; Henbest, K.; Fu, K.; Huang, W.; Lin, Y.; Taylor, S.; Carroll, D. L. *Chem. Phys. Lett.* **2002**, *351*, 349−353.

(28) Guldi, D. M.; Holzinger, M.; Hirsch, A.; Georgakilas, V.; Prato, M. *Chem. Commun.* **2003**, *10,* 1130−1131.

(29) O'Connell, M. J.; Bachilo, S. M.; Huffman, C. B.; Moore, V. C.; Strano, M. S.; Haroz, E. H.; Rialon, K. L.; Boul, P. J.; Noon, W. H.; Kittrell, C.; Ma, J.; Hauge, R. H.; Weisman, R. B.; Smalley, R. E. *Science* **2002**, *297*, 593−596.

(30) Lin, Y.; Rao, A. M.; Sadanadan, B.; Kenik, E. A.; Sun, Y.-P. *J. Phys. Chem. B* **2002**, *106*, 1294−1298.

(31) Fu, K.; Huang, W.; Lin, Y.; Riddle, L. A.; Carroll, D. L.; Sun, Y.-P. *Nano Lett.* **2001**, *1*, 439−441.

(32) Pimenta, M. A.; Marucci, A.; Empedocles, S. A.; Bawendi, M. G.; Hanlon, E. B.; Rao, A. M.; Eklund, P. C.; Smalley, R. E.; Dresselhaus, G.; Dresselhaus, M. S. *Phys. Rev. B* **1998**, *58*, R16016.

(33) (a) Dalton, A. B.; Stephan, C.; Coleman, J. N.; McCarthy, B.; Ajayan, P. M.; Lefrant, S.; Bernier, P.; Blau, W. J.; Byrne, H. J. *J. Phys. Chem. B* **2000**, *104*, 10012−10016. (b) Star, A.; Stoddart, J. F.; Diehl, M.; Boukai, A.; Wong, E. W.; Yang, X.; Chung, S. W.; Choi, H.; Heath, J. R. *Angew. Chem. Int. Ed*. **2001**, *40*, 1721−1725.

(34) Fernando, K. A. S.; Lin, Y.; Wang, W.; Kumar, S.; Zhou, B.; Xie, S.-Y.; Cureton, L. T.; Sun, Y.-P. *J. Am. Chem. Soc*. **2004**, *126*, 10234−10235.

MA0509210